J Neuropathol Exp Neurol

Vol. 73, No. 1
January 2014
pp. 30–38

ORIGINAL ARTICLE

Argyrophilic Grains Are Reliable Disease-Specific Features of Corticobasal Degeneration

Shinsui Tatsumi, MD, Maya Mimuro, MD, PhD, Yasushi Iwasaki, MD, PhD, Ryosuke Takahashi, MD, PhD, Akiyoshi Kakita, MD, PhD, Hitoshi Takahashi, MD, PhD, and Mari Yoshida, PhD, MD

Abstract

Argyrophilic grains are discrete punctate structures that bind to silver stains; they can be observed within the neuropil of the limbic system, particularly in the elderly. It has been reported that argyrophilic grains are more frequent in patients with corticobasal degeneration (CBD) compared with the elderly population in general. To determine the frequency and significance of argyrophilic grains in CBD, we examined the temporal lobes from 35 patients with autopsy-proven CBD (mean age, 69.1 years) and 28 patients with argyrophilic grain disease (mean age, 95.7 years). Grain distributions and densities were evaluated semiquantitatively using Gallyas-Braak stains and immunohistochemistry with AT8 and RD4 antibodies. Argyrophilic grains were observed in all CBD cases (100%) despite a lower average age at death in this population. We also observed the following features that were specific to argyrophilic grains in CBD: 1) grains were likely to be widespread throughout the temporal lobe, 2) grains were consistently found with abundant argyrophilic threads, and 3) the ultrastructure of grains contained paired helical filaments with a periodicity of 120 to 130 nm. In conclusion, we confirm that argyrophilic grains in CBD are specifically related to the 4-repeat tau pathology of CBD and are not simply a result of aging.

Key Words: Argyrophilic grain, Corticobasal degeneration, 4-repeat tauopathy, Tau.

INTRODUCTION

Argyrophilic grains are morphologically well-defined punctate structures that bind to silver stains (i.e. argyrophilic) and are primarily found within the limbic areas of the brain (1–5). More specifically, these roundish spindle- or comma-shaped lesions can best be detected using the Gallyas-Braak silver stain (1, 2). Argyrophilic grains are abnormal dendritic accumulations of phosphorylated tau proteins, which are mainly composed of tau isoforms with 4 microtubule-binding repeats (6–9).

Argyrophilic grain disease (AGD) is a late-onset condition in which argyrophilic grains are abundantly present within the medial temporal lobe (1–5); this disease is often accompanied by clinical manifestations such as cognitive decline and emotional changes (2, 5, 10, 11). The incidence of AGD is significantly correlated with increased age and was found to be as high as 30% to 40% in very old patients (11–13). It has also been reported that argyrophilic grains are frequently observed in corticobasal degeneration (CBD) (9, 14).

Corticobasal degeneration is a progressive neurodegenerative disorder that affects the cerebral cortex and various subcortical structures, including the basal ganglia and the substantia nigra (15–17). In CBD patients, immunohistochemistry shows widespread tau-positive inclusions such as pretangles, astrocytic plaques, coiled bodies, and argyrophilic threads, involving both neurons and glia (18–23). In contrast to AGD, the limbic system and other temporal lobe structures are more likely to be preserved than the frontal lobe in CBD, and the mean age of death is lower (e.g. reported as 69.5 years and 71.7 years) (14, 17, 24). Argyrophilic grains are reported to be more frequent in CBD patients than even in very old populations (57.7% vs. 30%–40%, respectively) (11–14).

Therefore, it is possible that the increased frequency of argyrophilic grains in CBD patients may be caused by factors other than aging. To our knowledge, however, there have been no reports addressing this problem. The aim of the current study is to establish the frequency and significance of argyrophilic grains in CBD patients by examining temporal lobe lesions in a large cohort of autopsy-proven CBD cases.

MATERIALS AND METHODS

Patients

We examined 35 autopsy cases with the neuropathologic diagnosis of CBD. These patients were chosen from the files of the Institute for Medical Science of Aging, Aichi Medical University, between 1983 and 2012 (Group A) and

From the Department of Neuropathology, Institute for Medical Science of Aging, Aichi Medical University, Aichi (ST, MM, YI, MY); Department of Neurology, Kyoto University, Kyoto (RT); and Department of Pathology, Brain Research Institute, Niigata University, Niigata (AK, HT), Japan.

Send correspondence and reprint requests to: Mari Yoshida, PhD, MD, Department of Neuropathology, Institute for Medical Science of Aging, Aichi Medical University, 1-1 Yazakokarimata, Nagakute, Aichi, 480-1195, Japan; E-mail: myoshida@aichi-med-u.ac.jp

This work was supported by the Collaborative Research Project (No. 2308) of the Brain Research Institute, University of Niigata, and by grants-in-aid from the Research Committee of CNS Degenerative Diseases, the Ministry of Health, Labour and Welfare of Japan.

Supplemental digital content is available for this article. Direct URL citations appear in the printed text and are provided in the HTML and PDF versions of this article on the journal's Web site (www.jneuropath.com).

TABLE. Demographic Features of Corticobasal Degeneration and Argyrophilic Grain Disease Patients

Demographic Feature	Group A (CBD)	Group B (CBD)	Total Cases With CBD	AGD Cases
No. cases	27	8	35	28
Sex (male/female)	19/8	4/4	23/12	6/22
Age at onset, (range), years	62.3 ± 7.5 (51–79)	65.0 ± 7.6 (58–81)	62.9 ± 7.4 (51–81)	na
Disease duration (range), years	5.3 ± 2.4 (2.7–10.4)	7.0 ± 3.7 (4.5–15.3)	5.7 ± 2.8 (2.7–15.3)	na
Age at death (range), years	68.2 ± 7.6 (54–86)	72.1 ± 7.4 (65–86)	69.1 ± 7.6 (54–86)	95.7 ± 11.6 (64–116)
Brain weight, g	1,134 ± 152 (770–1,400)	1,020 ± 107 (850–1,150)	1,107 ± 150 (770–1,400)	1,060 ± 155 (845–1,440)

AGD, argyrophilic grain disease; CBD, corticobasal degeneration; na, not applicable.

from the Brain Research Institute, Niigata University, between 1990 and 2011 (Group B). The demographic features of all CBD cases are summarized in the Table. Corticobasal degeneration diagnoses were based on previously reported criteria (17).

To compare the distributions of argyrophilic grains between CBD and AGD in detail, we examined 28 autopsy cases of AGD without other neurodegenerative disorders (Table). We further examined 30 cases of Alzheimer disease (AD) confirmed at autopsy (mean age at death, 89.3 ± 11.7 years; mean Braak neurofibrillary tangle [NFT] stage, 5.0 ± 0.7) and 30 cases of progressive supranuclear palsy (PSP) (mean age at death, 74.2 ± 9.8 years; mean Braak NFT stage, 1.5 ± 0.6). We compared the frequency and distribution of the grains among these conditions with those in CBD cases.

Routine Neuropathology

Brain samples were fixed in 20% buffered or nonbuffered formalin for several weeks, and coronal slices were prepared. Multiple sections of the temporal lobes were obtained from paraffin-embedded samples, including regions of the temporal pole, the amygdala, and the anterior and posterior hippocampus; both sides of the temporal lobes were investigated when possible. Nine-micrometer-thick sections were stained with hematoxylin and eosin, Kluver-Barrera, and Gallyas-Braak (25) stains.

Immunohistochemistry

Serial 4.5-μm-thick sections were used for immunohistochemistry. The following primary antibodies were used to stain all temporal lobe sections: anti–phosphorylated tau (AT8, monoclonal, 1:3500; Innogenetics, Zwijindrecht, Belgium), anti–human 3-repeat tau (RD3, monoclonal, 1:3000; Upstate, Lake Placid, NY), and anti–human 4-repeat tau (RD4, monoclonal, 1:700; Upstate). For select sections, anti–amyloid β protein (6F/3D, monoclonal, 1:100; Dako, Glostrup, Denmark), anti–phosphorylated α-synuclein (pSyn No. 64, monoclonal, 1:3500; Wako, Osaka, Japan), and antineurofilament (2F11, monoclonal, 1:600; Dako) antibodies were also used. For RD3 and RD4 immunostaining, deparaffinized sections were retrieved in 3 mmol/L citric acid (pH 6.0) at 98°C for 40 minutes and were then pretreated in 98% formic acid for 20 minutes. All sections were immersed in 3% H_2O_2 for 10 minutes before antibody incubation. After incubation with the primary antibodies for 2 hours, the sections were treated with Envision-plus Peroxidase (Dako) for 60 minutes, and peroxidase labeling was detected with a solution containing 0.05 mg/mL 3,3′-diaminobenzidine (Wako). The immunolabeled sections were lightly counterstained with hematoxylin.

Double Immunofluorescence Staining of Grains in CBD

Nine-micrometer-thick sections from the hippocampus and temporal neocortex were incubated with a mixture of anti-tau (Tau, rabbit, polyclonal, 1:600; Dako) and anti–microtubule-associated protein 2 ([MAP2] HM-2, mouse, monoclonal, 1:100; Sigma-Aldrich, St. Louis, MO) antibodies. Anti-mouse antibody conjugated to Alexa Fluor 488 (1:200; Molecular Probes) and an anti-rabbit antibody conjugated to Alexa Fluor 568 (1:200; Molecular Probes) were used as secondary antibodies. Sections were also stained with anti-tau (Tau, 1:600; Dako) and anti–glial fibrillary acidic protein ([GFAP] 6F2, mouse, monoclonal; 1:80; Dako). For these immunofluorescence stainings, the deparaffinized sections were retrieved in 3 mmol/L citric acid (pH 6.0) at 98°C for 30 minutes. These sections were observed using

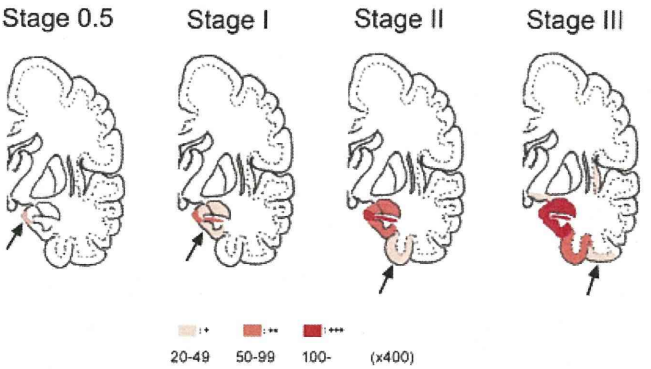

FIGURE 1. Stage classifications based on the topographic distributions of the argyrophilic grains in coronal sections through the amygdala. Stage 0.5, grains are located within the ambient gyrus and hippocampus; stage I, abundant grains (≥20 grains per 400× field of view) spread into the parahippocampal area; stage II, abundant grains spread into the occipitotemporal gyrus; stage III, abundant grains spread into the inferior aspect of the inferior temporal gyrus. This figure is modified from Figure 1 in the study of Saito et al (11) and reproduced with permission from the *Journal of Neuropathology and Experimental Neurology*.

fluorescence confocal microscopy (LSM 710; Carl Zeiss, Oberkochen, Germany).

Immunoelectron Microscopy

Electron microscopic observations were performed using formalin-fixed brains (i.e. the hippocampus and limbic cortex). We used the pre-embedding Q-dots immunolabeling, which was modified from the previously reported method (26). Thirty-micrometer-thick free-floating sections were incubated in anti–phosphorylated tau antibody (AT8, 1:700) for 24 hours, and an anti–mouse IgG antibody conjugated to Q-dot 655 (1:700, goat; Invitrogen, Carlsbad, CA) was used as a secondary antibody (for 8 hours). These sections were then fixed in 2% glutaraldehyde, postfixed in 1% OsO_4, and embedded in Epon. Ultrathin sections were stained with uranyl acetate and lead citrate and then examined with a JEM-1400 electron microscope (JEOL, Tokyo, Japan).

Analysis of Argyrophilic Grains

The density and distribution of argyrophilic grains were semiquantitatively estimated (Figs. 1, 2). Density scoring was based on the number of grains within a 400× field of view of a Gallyas-Braak–stained sample: +/−, 10 to 19; 1+, 20 to 49; 2+, 50 to 99; and 3+, greater than or equal to 100 (Fig. 2). Scores were determined for the amygdala, the hippocampus (the subiculum, the CA1–CA3 regions, and the dentate gyrus), the parahippocampal gyrus, and each gyrus of the temporal neocortex (the occipitotemporal gyrus and the inferior, middle, and superior temporal gyri). We separated the grain distribution patterns into 4 subgroups: stage 0.5, grains were localized to the ambient gyrus and to the transition area of the subiculum/CA1 region of the hippocampus; stage I, abundant grains (≥20 grains per 400× field of view) spread into the anterior parahippocampal area; stage II, abundant grains spread into the occipitotemporal gyrus; and stage III, abundant grains spread into the inferior aspect of the inferior temporal gyrus (Fig. 1). These stages were modified from those of Saito et al (11).

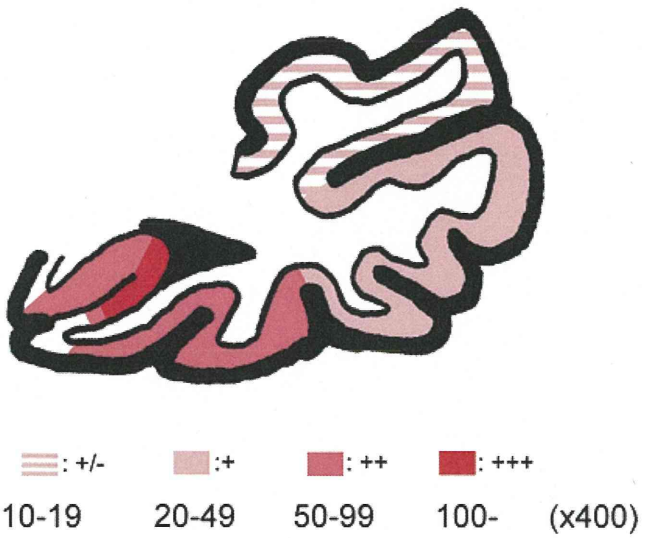

FIGURE 2. Representative image of grain density scoring. The density of argyrophilic grains in each brain region was semiquantitatively determined within 400× fields of view of Gallyas-Braak–stained sections. Density scoring categories were as follows: +/-, 10 to 19; +, 20 to 49; ++, 50 to 99; +++, greater than or equal to 100.

Analysis of Argyrophilic Threads in the Anterior Hippocampus

To clarify the relationship between argyrophilic grains and argyrophilic threads, we classified the density of argyrophilic threads into 3 grades in Gallyas-Braak–stained samples of the anterior hippocampus as follows: grade 1+, argyrophilic threads in the hippocampus were not visible to the naked eye, but a small number of threads were found microscopically in the CA1 region and the subiculum of the hippocampus; grade 2+, argyrophilic threads were visible to the naked eye in the area between the alveus hippocampi and the hippocampal pyramidal cell layer, and a moderate amount of argyrophilic threads were observed microscopically; and grade 3+, argyrophilic threads were visible to the naked eye throughout the hippocampus, including the hippocampal pyramidal and molecular layers, and a large amount of argyrophilic threads were observed microscopically (Fig. 3).

Morphologic Differentiation Between Argyrophilic Grains and Threads

In CBD, argyrophilic grains are usually accompanied by argyrophilic threads, and it is often difficult to distinguish between them. Here, we identified the grains by their well-defined round shape and the threads by their thin and curled shapes. To verify this, we also stained 30-μm-thick sections from select cases with Gallyas-Braak stain and compared these with the 9-μm-thick sections. Examination of the 30-μm-thick sections showed that argyrophilic threads were usually thin (<1 μm in thickness), elongated, curled, and visible along their entire lengths. Under microscopy, either end of the threads may be out of focus. Conversely, the grains tended to be thick (i.e. 2–5 μm in thickness), short, and ovoid, with clear margins. Similar results were also observed in the 9-μm-thick sections with Gallyas-Braak staining (Fig. 4).

Some grains possessed a threadlike short tail, but the grains connected to longer argyrophilic threads were rare in both AGD and CBD cases. The frequency of the former grain type was similar in both conditions (~20% of the total grains). In CBD, there was another difference between the argyrophilic grains and threads. In the cerebral cortex, the grains were almost exclusively located in the superficial layers (i.e. Layers II and III), but the threads were distributed in both the superficial and deep layers. The argyrophilic grains were absent in the white matter. Based on these grain findings (i.e. rounded shape, clear margin, and characteristic distribution in the cortical layers), we concluded that the argyrophilic grains and threads could be discerned in both the 9-μm- and 30-μm-thick sections.

Statistical Analysis

Spearman correlation calculations were used to determine the relationships between grain stage and age of onset, age at death, disease duration, brain weight, and density of argyrophilic

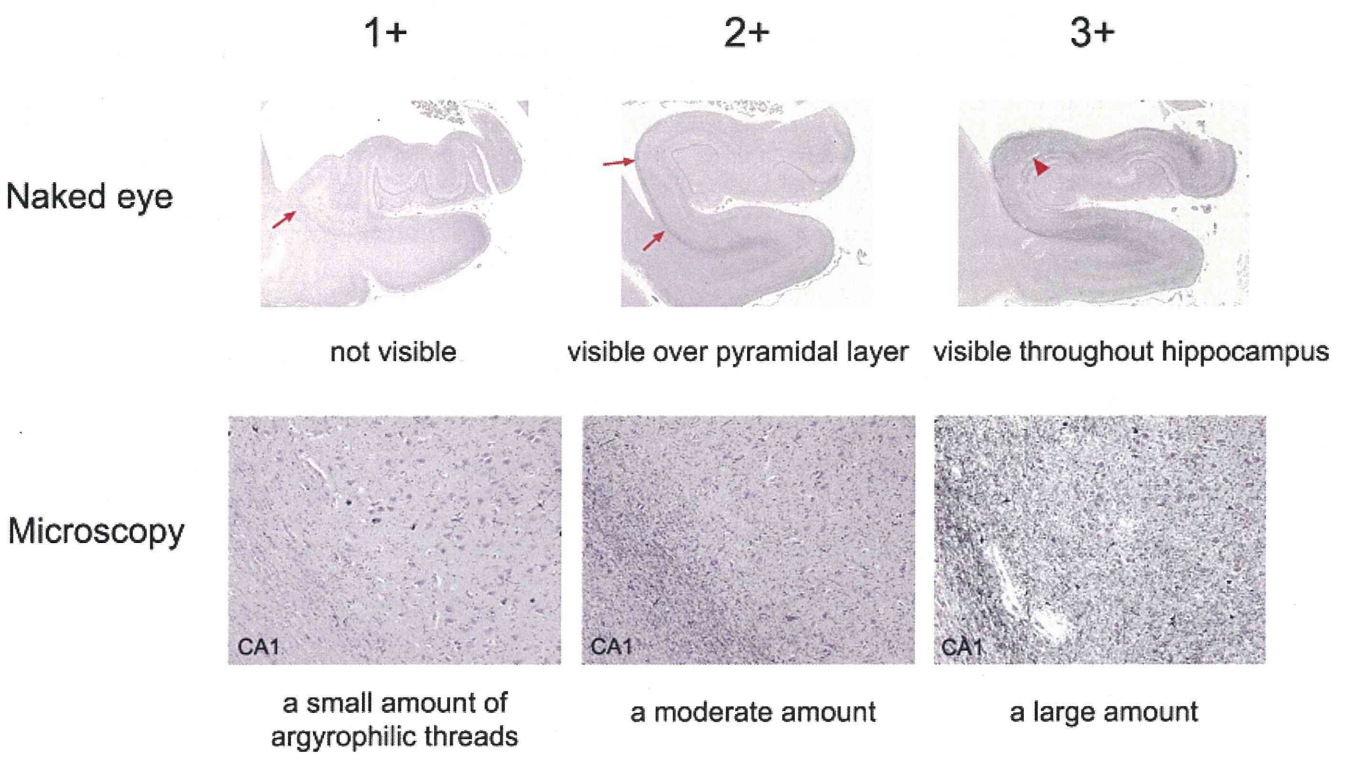

FIGURE 3. Gallyas-Braak–stained argyrophilic threads within the anterior hippocampus. Grading scores were as follows: 1+, argyrophilic threads in the hippocampus not visible to the naked eye, but small numbers of threads could be observed microscopically; 2+, argyrophilic threads were visible to the naked eye in the area between the alveus hippocampi and the hippocampal pyramidal cell layer (arrows), and microscopy revealed a moderate number of threads; 3+, argyrophilic threads were widespread throughout the hippocampus and visible to the naked eye within the hippocampal pyramidal layer (arrowhead), and large numbers of threads could be observed microscopically.

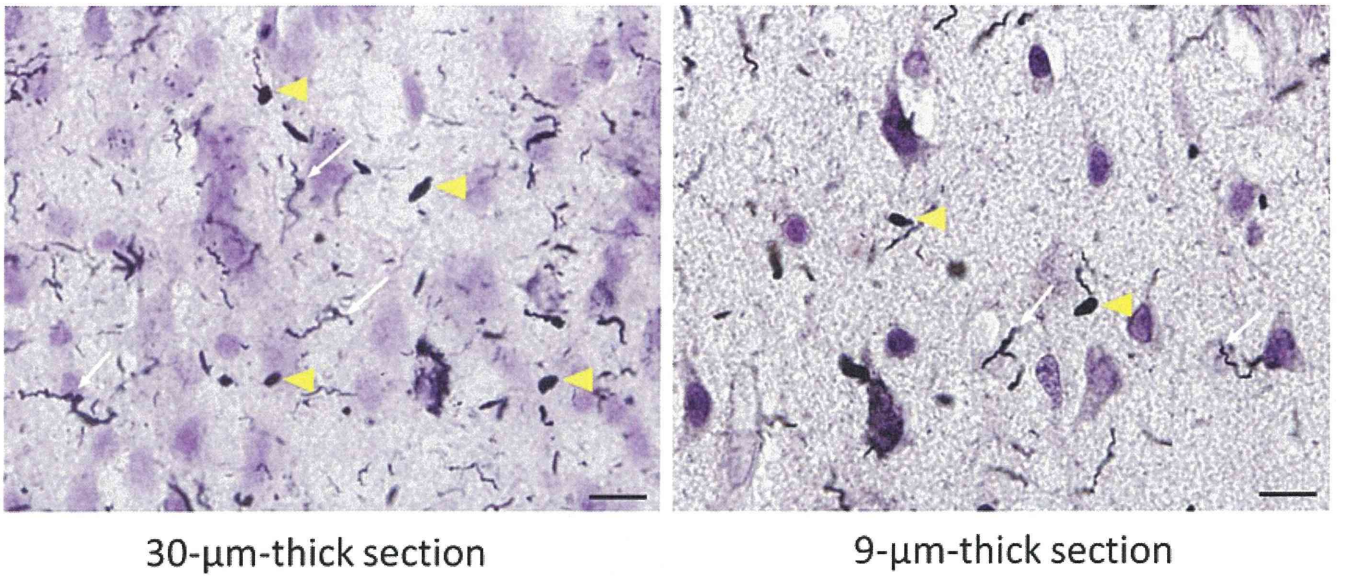

FIGURE 4. Differentiation between argyrophilic grains and argyrophilic threads in Gallyas-Braak–stained samples in the superficial layer of the middle temporal gyrus. In 30-µm-thick sections, argyrophilic threads (arrows) are observed along their entire lengths without interruption. Compared with argyrophilic grains, the argyrophilic threads are curled and thinner and they lack a round morphology. Therefore, argyrophilic threads could be readily differentiated from grains (arrowheads). Similar results were obtained from 9-µm-thick sections. Scale bar = 10 µm.

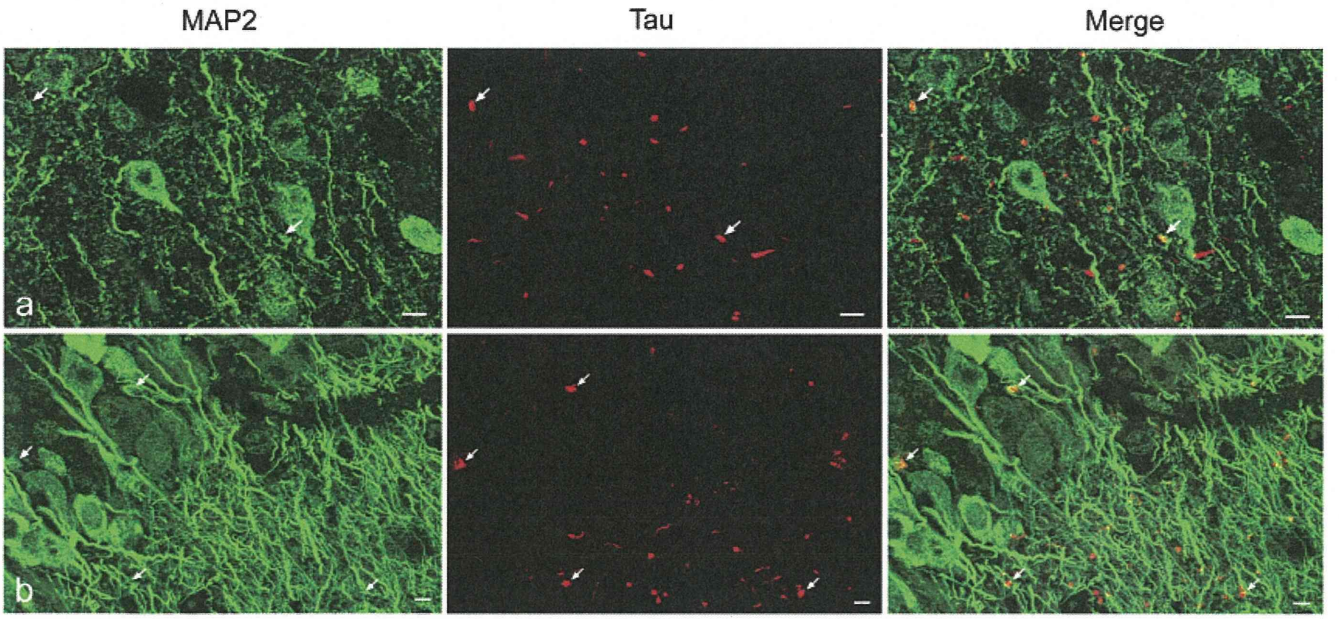

FIGURE 5. Double immunofluorescence staining of dendrites and grains in the temporal neocortex and the hippocampal dentate gyrus in corticobasal degeneration (CBD). Sections were double immunostained with mouse anti–microtubule-associated protein 2 (MAP2) and rabbit anti-tau antibodies. The primary antibodies were visualized with anti-mouse Alexa Fluor 488 (green) and anti-rabbit Alexa Fluor 568 (red). **(A)** Confocal images of the grains in the inferior temporal gyrus show colocalization of MAP2 and tau in some grains (arrows). **(B)** In the hippocampal dentate gyrus, the tau-positive grains occasionally showed continuity with the dendrites, which were labeled by anti-MAP2 (arrows). Scale bar = 5 μm.

threads. Statistical analyses were performed using the Mann-Whitney U test for a nonparametric analysis. The results were considered statistically significant when $p < 0.05$.

RESULTS

Double Immunofluorescence Staining of Grains in CBD

Double immunofluorescence staining showed that the tau-positive grains in the cerebral cortex were occasionally colocalized with MAP2 (Fig. 5A). Some grains also showed continuity with the MAP2-positive dendrites (Fig. 5B, hippocampal dentate gyrus). The astrocytes stained with anti-GFAP were not related to the tau-positive grains. These findings suggested that the grains in CBD were related to dendrites, which was similar to observations of grains in AGD (8).

Frequency and Density of Argyrophilic Grains in CBD

Argyrophilic grains were observed in all cases with CBD (Fig. 6). In 9 cases (25.7%), grains were observed within the amygdala and hippocampus (Stage 0.5). Notably, grain stage III was the most common among all CBD cases (11 cases or 31.4%), suggesting that argyrophilic grains were likely widely distributed in CBD. The mean grain stage was 1.8 ± 1.0. Asymmetry in grain stage between the 2 temporal lobes was noted in 68.8% of cases (11 of the 16 cases in which grain stage data were available from both sides). In contrast to the severity of the grains, the NFT Braak stages were generally mild (mean, 1.5 ± 0.7). Moreover, the NFT distributions were atypical in approximately 40% of cases. The NFTs were rarely accompanied by neuropil threads, as is common in AD, and the NFTs were in combination with numerous pretangles (Figure, Supplemental Digital Content 1, http://links.lww.com/NEN/A538); in these cases, the 4-repeat tau isoform was more common than the 3-repeat isoform by immunohistochemistry. In the limbic system, gliosis that is often associated with argyrophilic grains was generally mild and, in most cases, neuronal loss was not

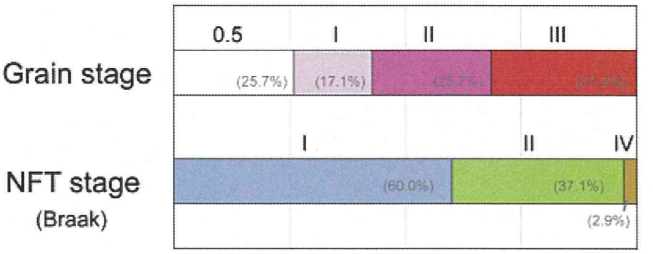

FIGURE 6. The frequency of argyrophilic grains and neurofibrillary tangles (NFTs) in corticobasal degeneration (CBD). Argyrophilic grains were observed in all cases of CBD (n = 35). Notably, grain stage III was most common, suggesting that grains are widespread in CBD patients. In contrast to the severity of the grains, the NFT Braak stages were generally mild. The distributions of the grains were classified into 4 stages: stage 0.5, grains were localized to the limbic system; stages I and II, abundant grains spread into the parahippocampal and occipitotemporal gyri, respectively; and stage III, abundant grains were diffusely and widely distributed, reaching to the inferior temporal gyrus.

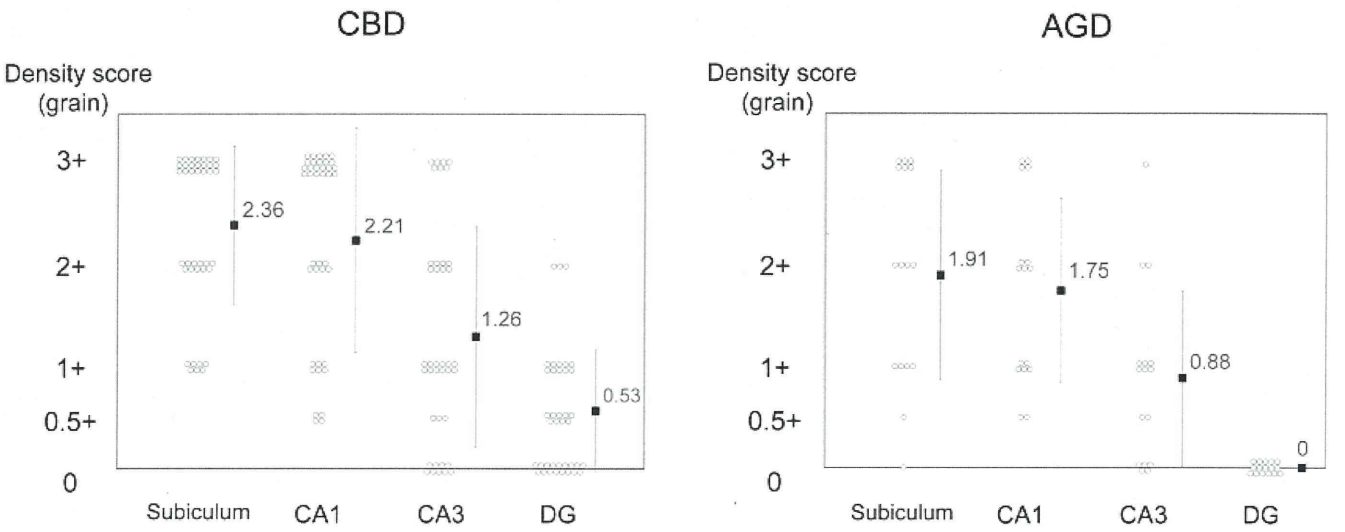

FIGURE 7. Topographic distributions of the argyrophilic grains within the anterior hippocampus in corticobasal degeneration (CBD) vs. argyrophilic grain disease (AGD). Argyrophilic grains were abundant in the subiculum and in the CA1 and CA3 regions of the hippocampus in both diseases. Grains in the hippocampal dentate gyrus (DG) were significantly more frequent in CBD than in AGD (Mann-Whitney *U* -test, p = 0.0011). When possible, both sides of the anterior hippocampus were examined; n = 39 for CBD and n = 16 for AGD. Density scoring of the grains was semiquantitatively determined in 400× fields-of-view of Gallyas-Braak-stained samples; density scoring categories were as follows: 0.5+ = 10 to 19; 1+ = 20 to 49; 2+ = 50 to 99; 3+ = ≥100. Bars represent SE.

observed. Even in CBD cases with grain stage III, neuronal loss within the amygdala was only slight to mild.

The Topographic Distribution of Argyrophilic Grains Within the Anterior Hippocampus

Within the anterior hippocampus, argyrophilic grains were most frequently observed in the subiculum, the CA1 region, and the CA3 region (in decreasing order) in both CBD and AGD (Fig. 7). Very few grains were observed in the dentate gyrus of the hippocampus in AGD cases. By contrast, in as many as 15 of the 35 CBD cases, more than 10 grains were observed per 400× microscopic field of view in the hippocampal dentate gyrus. Within the dentate gyrus, grains were most frequently observed in the molecular layer (Fig. 8). Grain density in the dentate gyrus was significantly higher in CBD than in AGD (Mann-Whitney U test, $p < 0.0011$).

The Topographic Distribution of Argyrophilic Grains Within the Temporal Neocortex

In AGD, argyrophilic grains were rarely observed beyond the inferior aspect of the inferior temporal gyrus, and grain density decreased sharply based on distance from the limbic

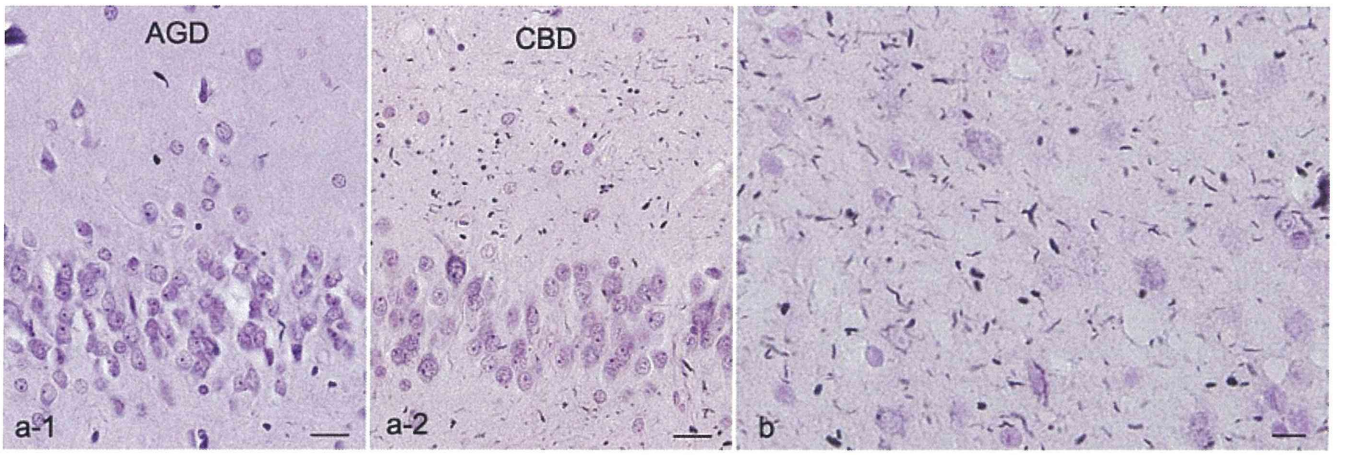

FIGURE 8. Uncommon distributions of argyrophilic grains within the temporal lobe. **(A)** Grains were very rarely observed within the dentate gyrus in argyrophilic grain disease (AGD) **(A-1)**; however, grains were sometimes observed in the molecular layer of the dentate gyrus in corticobasal degeneration (CBD) **(A-2)**. **(B)** Grains could also be found widely distributed throughout the temporal neocortex (the superficial layer of the superior temporal gyrus). Gallyas-Braak–stained samples. Scale bar = 20 μm.

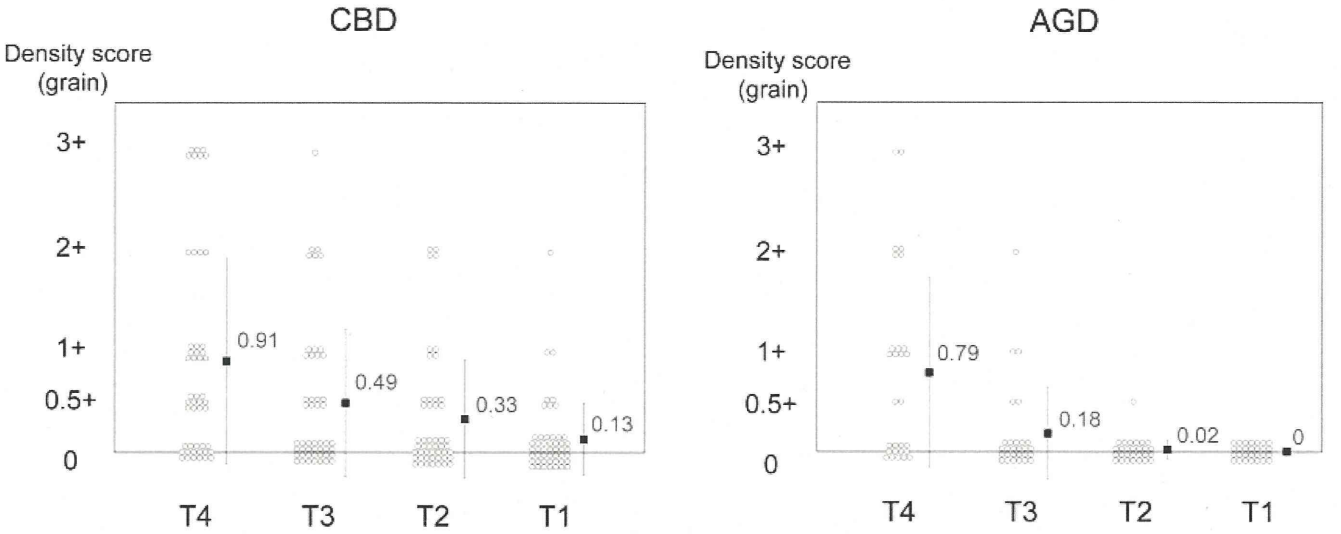

FIGURE 9. Topographic distributions of argyrophilic grains within the temporal neocortex in corticobasal degeneration (CBD) versus argyrophilic grain disease (AGD). In most AGD cases, grains were not observed beyond the inferior temporal gyrus. In contrast, grains could be observed in the middle and superior temporal gyri in CBD. In the middle temporal gyrus, grains were significantly more frequent in CBD than in AGD (Mann-Whitney U test, $p < 0.05$). When possible, both sides of the anterior hippocampus were examined; n = 49 for CBD and n = 28 for AGD. Density scoring of the grains was semiquantitatively determined in 400× fields of view of Gallyas-Braak–stained samples. Density scoring categories were as follows: 0.5+, 10 to 19; 1+, 20 to 49; 2+, 50 to 99; 3+, greater than or equal to 100. T1, T2, T3, and T4 denote the superior, middle, and inferior temporal gyri and the occipitotemporal gyrus, respectively. Bars represent SE.

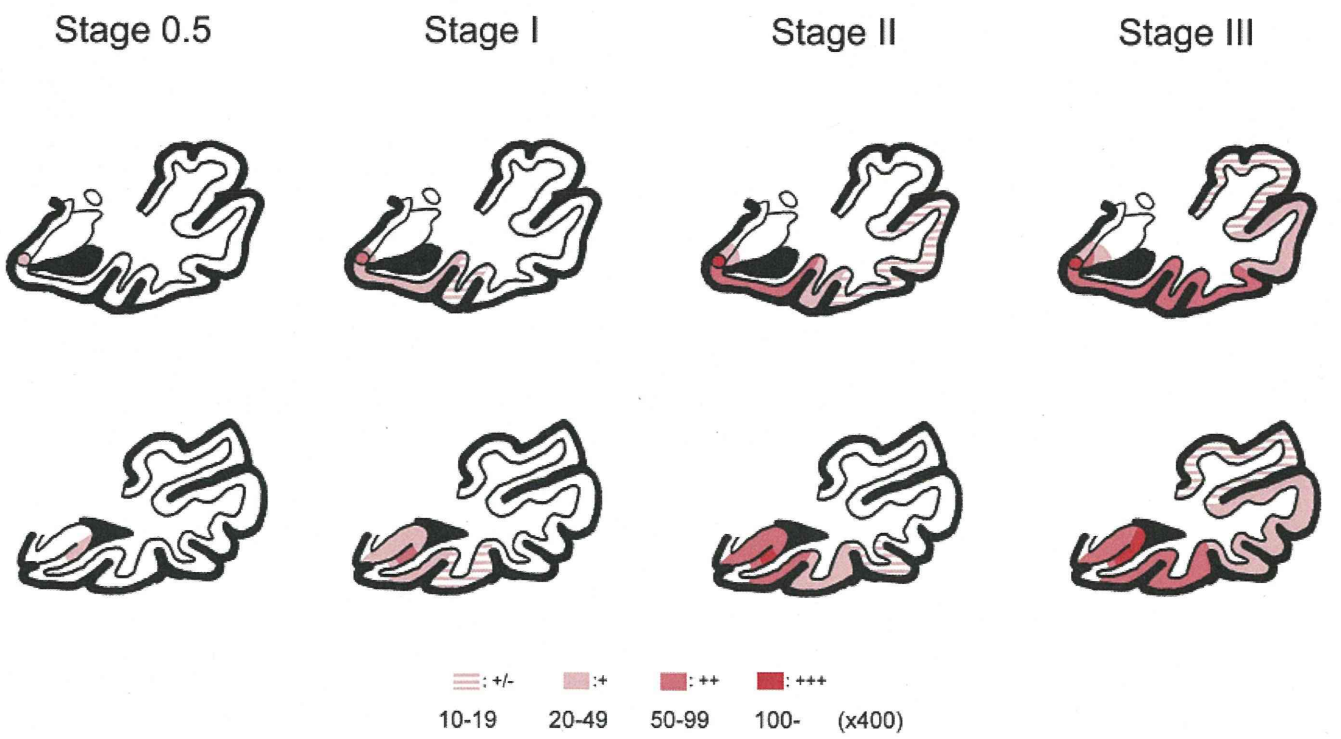

FIGURE 10. Illustrations of the topographic distributions of the argyrophilic grain stages. In grain stage 0.5, grains were limited to the most vulnerable areas of the limbic system. In stages II and III, small numbers of argyrophilic grains were more widely distributed, spreading to the lateral aspects of the temporal lobe.

system (Fig. 9). In contrast, in some CBD cases, grains were observed in the lateral aspect of the temporal lobe (Figs. 8, 9). Grain density scores in the middle temporal gyrus were significantly higher in CBD than in AGD (Mann-Whitney U test, $p < 0.05$). The argyrophilic grain distributions for each grain stage clearly show a tendency for small numbers of grains that are widely distributed throughout the temporal lobe in CBD (Fig. 10).

The Prevalence of Argyrophilic Threads Within the Anterior Hippocampus

Similar to argyrophilic grains, argyrophilic threads were observed within the anterior hippocampus in all CBD cases. Furthermore, argyrophilic thread grade was significantly correlated with argyrophilic grain stage in the anterior hippocampus (Spearman rank correlation coefficient, $p < 0.0001$, $p = 0.65$) (Fig. 11).

Finally, brain weight was also significantly associated with grain stage (Spearman rank correlation coefficient, $p < 0.01$), but other factors, such as age of onset, age at death, and disease duration, were not correlated with grain stage ($p = 0.13$, 0.12, and 0.10, respectively) (Table).

The Frequency and Distribution of Grains in AD and PSP

Grains were observed in 36.7% of the AD patients (11 of 30 cases: stage 0.5, 3 cases; stage 1, 5 cases; stage 2, 1 case; and stage 3, 2 cases). In PSP cases, grains were present in 26.7% of the patients (8 of 30 cases: stage 0.5, 1 cases; stage 1, 7 cases). The finding of widespread grain distribution in CBD (i.e. lateral aspects of the temporal lobe and hippocampal dentate gyrus) was not observed in either the AD or PSP patients.

Electron Microscopic Observations of the Grains in CBD

By electron microscopy, grains in the limbic cortex were spindle-shaped aggregations of straight and paired helical filaments (PHFs) (Fig. 12). The straight tubules measured 12 to 15 nm in diameter, and the periodicity of the PHFs was 120 to 130 nm (Fig. 12). The AT8-positive tau filaments were immunolabeled with Q-dots and more densely labeled in the outer portions of grains. Similar findings were observed in the hippocampal dentate gyrus.

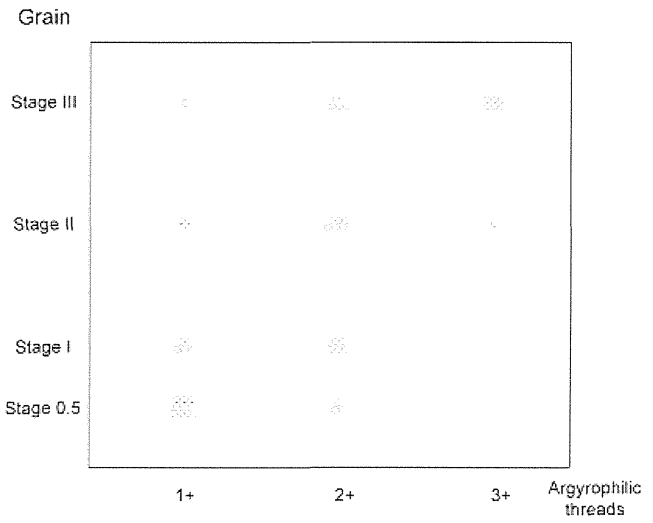

FIGURE 11. Correlation between the prevalence of argyrophilic threads and grain stages ($p < 0.0001$, Spearman $\rho = 0.65$).

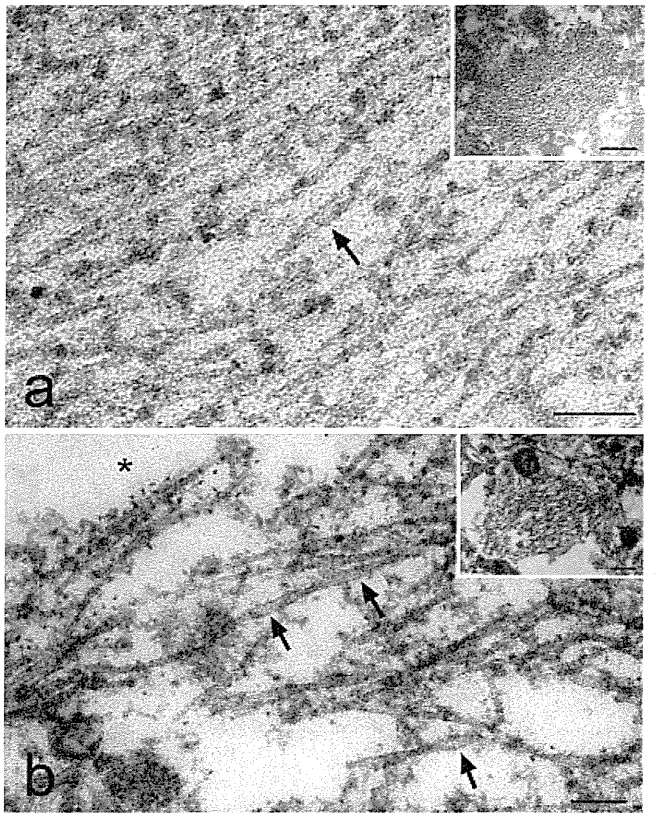

FIGURE 12. Grain ultrastructure in corticobasal degeneration (CBD). **(A)** A grain in the hippocampal dentate gyrus from a 77-year-old man with CBD contains a bundle of straight and most likely twisted tubules, which are intermixed with ribosomes. **(B)**. A grain in the limbic lobe of a 70-year-old woman with CBD contains paired helical filaments with a long periodicity (120–130 nm). The straight tubules measure 12 to 15 nm in diameter. The AT8-positive tau filaments are densely immunolabeled with Q-dots (an asterisk; 10-nm particles with a peripheral halo). The insets show a low-power view of spindle-shaped grains. Scale bars = 100 nm; (insets) 500 nm.

DISCUSSION

Previous reports have shown that argyrophilic grains are common in cases of CBD (e.g. 41.2% and 57.7%) (9, 14); the prevalence in the present study was much higher (100%). It may be difficult to distinguish between argyrophilic grains and argyrophilic threads because both are small and show argyrophilic properties; and they are usually intermingled with one another within the neuropil of the limbic area in CBD. To overcome the inherent challenges in distinguishing between argyrophilic grains and argyrophilic threads, we used thick sections (30 μm) with the Gallyas-Braak stain. Using this method, the thinner and curled argyrophilic threads could

be observed along their entire lengths without interruption and they were readily distinguishable from round punctate argyrophilic grains. Similar findings were obtained in the 9-μm-thick sections.

Importantly, we demonstrate that the argyrophilic grains observed in CBD patients are not merely a result of aging but are indeed correlated with CBD. This conclusion was based on a number of observations. First, the grain frequency was unexpectedly high (100%) in the CBD cases despite the relatively young age at death and low Braak AD NFT scores in these patients. Second, a tendency toward widespread grain distributions throughout the temporal lobe was only observed for the CBD cases. For example, in CBD cases with grain stages II and III, argyrophilic grains were often found in unusual areas, including the lateral aspects of the temporal cortex and the molecular layer of the hippocampal dentate gyrus. This characteristic distribution was not observed in patients with AGD, including cases of coexistent AD or PSP pathology. Finally, in CBD cases, grain stage was significantly associated with the density of argyrophilic threads within the anterior hippocampus. This association between grains and abundant argyrophilic threads may be indicative of CBD because it was never observed in the AGD cases.

By electron microscopy, the grains in CBD were composed of aggregations of 12- to 15-nm straight filaments and PHFs with a periodicity of 120 to 130 nm. These findings were consistent with earlier observations of neuronal inclusions in CBD (20, 23, 27, 28). In contrast, the grains in the aging processes were composed of 9- to 19-nm straight filaments, and PHFs have not been reported (2, 4, 8). Therefore, the presence of PHFs with a longer periodicity suggests that the grains in CBD are mechanistically different from the grains in human aging processes.

It is debatable whether grains in CBD are a distinct CBD pathology. Compared with other CBD pathologies, the grains in CBD were most frequently observed in the medial temporal structures (i.e. a limbic-predominant pattern). This observation is different from the "perirolandic" or "parasagittal" pattern of gross and microscopic lesions in CBD (17). Moreover, in light of the distribution in the cerebral cortex, the grains were located almost exclusively in the superficial layers (Layers II and III), whereas the threads were distributed in both the superficial and deep layers. Thus, the grains in CBD are not simply part of a spectrum of other CBD pathologies, but they are a distinct pathology in CBD.

In conclusion, we show that the argyrophilic grains in CBD cases are closely related to the 4-repeat tau pathology of CBD and are not simply a result of aging. They may represent 1 characteristic pathologic feature of CBD.

REFERENCES

1. Braak H, Braak E. Argyrophilic grains: Characteristic pathology of cerebral cortex in cases of adult onset dementia without Alzheimer changes. Neurosci Lett 1987;76:124–27
2. Braak H, Braak E. Cortical and subcortical argyrophilic grains characterize a disease associated with adult onset dementia. Neuropathol Appl Neurobiol 1989;15:13–26
3. Braak H, Braak E. Argyrophilic grain disease: Frequency of occurrence in different age categories and neuropathological diagnostic criteria. J Neural Transm 1998;105:801–19
4. Tolnay M, Spillantini MG, Goedert M, et al. Argyrophilic grain disease: Widespread hyperphosphorylation of tau protein in limbic neurons. Acta Neuropathol 1997;93:477–84
5. Tolnay M, Schwietert M, Monsch AU, et al. Argyrophilic grain disease: Distribution of grains in patients with and without dementia. Acta Neuropathol 1997;94:353–58
6. Schultz C, Koppers D, Sassin I, et al. Cytoskeletal alterations in the human tuberal hypothalamus related to argyrophilic grain disease. Acta Neuropathol 1998;96:596–602
7. Tolnay M, Mistl C, Ipsen S, et al. Argyrophilic grains of Braak: Occurrence in dendrites of neurons containing hyperphosphorylated tau protein. Neuropathol Appl Neurobiol 1998;24:53–59
8. Ikeda K, Akiyama H, Kondo H, et al. A study of dementia with argyrophilic grains: Possible cytoskeletal abnormality in dendrospinal portion of neurons and oligodendroglia. Acta Neuropathol 1995;89:409–14
9. Togo T, Sahara N, Yen S-H, et al. Argyrophilic grain disease is a sporadic 4-repeat tauopathy. J Neuropathol Exp Neurol 2002;61:547–56
10. Ikeda K, Akiyama H, Arai T, et al. Clinical aspects of argyrophilic grain disease. Clin Neuropathol 2000;19:278–84
11. Saito Y, Ruberu NN, Sawabe M, et al. Staging of argyrophilic grains: An age-associated tauopathy. J Neuropathol Exp Neurol 2004;63:911–18
12. Ding ZT, Wan Y, Jiang YP, et al. Argyrophilic grain disease: Frequency and neuropathology in centenarians. Acta Neuropathol 2006;111:320–28
13. Knopman DS, Parisi JE, Salviati A, et al. Neuropathology of cognitively normal elderly. J Neuropathol Exp Neurol 2003;62:1087–95
14. Kouri N, Murray ME, Hassan A, et al. Neuropathological features of corticobasal degeneration presenting as corticobasal syndrome or Richardson syndrome. Brain 2011;134:3264–75
15. Rebeiz JJ, Kolodny EH, Richardson EP. Corticodentatonigral degeneration with neuronal achromasia. Arch Neurol 1968;18:20–33
16. Gibb WRG, Luthert PJ, Marsden CD. Corticobasal degeneration. Brain 1989;112:1171–92
17. Dickson DW, Bergeron C, Chin SS, et al. Office of rare diseases neuropathologic criteria for corticobasal degeneration. J Neuropathol Exp Neurol 2002;61:935–46
18. Feany MB, Dickson DW. Widespread cytoskeletal pathology characterizes corticobasal degeneration. Am J Pathol 1995;146:1388–96
19. Mori H, Nishimura M, Namba Y, et al. Corticobasal degeneration: A disease with widespread appearance of abnormal tau and neurofibrillary tangles, and its relation to progressive supranuclear palsy. Acta Neuropathol 1994;88:113–21
20. Arima K, Uesugi H, Fujita I, et al. Corticonigral degeneration with neuronal achromasia presenting with primary progressive aphasia: Ultrastructural and immunocytochemical studies. J Neurol Sci 1994;127:186–97
21. Ikeda K, Akiyama H, Haga C, et al. Argyrophilic thread-like structure in corticobasal degeneration and supranuclear palsy. Neurosci Lett 1994;174:157–59
22. Yamada T, McGeer PL. Oligodendroglial microtubular masses: An abnormality observed in some human neurodegenerative diseases. Neurosci Lett 1990;120:163–66
23. Wakabayashi K, Oyanagi K, Makifuchi T, et al. Corticobasal degeneration: Epipathological significance of the cytoskeletal alterations. Acta Neuropathol 1994;87:545–53
24. Ling H, O'Sullivan SS, Holton JL, et al. Does corticobasal degeneration exist? A clinicopathological re-evaluation. Brain 2010;133:2045–57
25. Braak H, Braak E, Ohm T, et al. Silver impregnation of Alzheimer's neurofibrillary changes counterstained for basophilic and lipofuscin pigment. Stain Technol 1988;63:197–200
26. Uematsu M, Adachi E, Nakamura A, et al. Atomic identification of fluorescent Q-dots on tau-positive fibrils in 3D-reconstructed Pick bodies. Am J Pathol 2012;180:1394–97
27. Ksiezak-Reding H, Morgan K, Mattiace LA, et al. Ultrastructure and biochemical composition of paired helical filaments in corticobasal degeneration. Am J Pathol 1994;145:1496–1508
28. Takahashi T, Amano N, Hanihara T, et al. Corticobasal degeneration: Widespread argentophilic thread and glia in addition to neurofibrillary tangles. Similarities of cytoskeletal abnormalities in corticobasal degeneration and progressive supranuclear palsy. J Neurol Sci 1996;138:66–77

NEUROPATHOLOGY

Neuropathology 2014; **34**, 19–26 doi:10.1111/neup.12056

Original Article

ALS-associated protein FIG4 is localized in Pick and Lewy bodies, and also neuronal nuclear inclusions, in polyglutamine and intranuclear inclusion body diseases

Tomoya Kon,[1] Fumiaki Mori,[1] Kunikazu Tanji,[1] Yasuo Miki,[1] Yasuko Toyoshima,[2] Mari Yoshida,[4] Hidenao Sasaki,[5] Akiyoshi Kakita,[3] Hitoshi Takahashi[2] and Koichi Wakabayashi[1]

[1]Department of Neuropathology, Hirosaki University Graduate School of Medicine, Hirosaki, [2]Department of Pathology, Brain Research Institute, [3]Department of Pathological Neuroscience, Center for Bioresource-based Researches, University of Niigata, Niigata, [4]Department of Neuropathology, Aichi Medical University, Nagakute and [5]Department of Neurology, Hokkaido University Graduate School of Medicine, Sapporo, Japan

FIG4 is a phosphatase that regulates intracellular vesicle trafficking along the endosomal-lysosomal pathway. Mutations of *FIG4* lead to the development of Charcot-Marie-Tooth disease type 4J and amyotrophic lateral sclerosis (ALS). Moreover, ALS-associated proteins (transactivation response DNA protein 43 (TDP-43), fused in sarcoma (FUS), optineurin, ubiquilin-2, charged mutivesicular body protein 2b (CHMP2B) and valosin-containing protein) are involved in inclusion body formation in several neurodegenerative diseases. Using immunohistochemistry, we examined the brains and spinal cords of patients with various neurodegenerative diseases, including sporadic TDP-43 proteinopathy (ALS and frontotemporal lobar degeneration). TDP-43 proteinopathy demonstrated no FIG4 immunoreactivity in neuronal inclusions. However, FIG4 immunoreactivity was present in Pick bodies in Pick's disease, Lewy bodies in Parkinson's disease and dementia with Lewy bodies, neuronal nuclear inclusions in polyglutamine and intranuclear inclusion body diseases, and Marinesco and Hirano bodies in aged control subjects. These findings suggest that FIG4 is not incorporated in TDP-43 inclusions and that it may have a common role in the formation or degradation of neuronal cytoplasmic and nuclear inclusions in several neurodegenerative diseases.

Key words: endosomal-lysosomal pathway, FIG4, Lewy body, nuclear inclusion, Pick body.

Correspondence: Tomoya Kon, MD, Department of Neuropathology, Institute of Brain Science, Hirosaki University Graduate School of Medicine, 5 Zaifu-cho, Hirosaki 036-8562, Japan. Email: t-kon@umin.ac.jp

Received 8 June 2013; revised and accepted 25 June 2013; published online 29 July 2013.

INTRODUCTION

Factor-Induced-Gene 4 (FIG4), also known as *SAC3*, was first cloned from a human immature myeloid cell line in 1996.[1,2] The protein encoded by *FIG4* is a phosphatase that regulates phosphatidylinositol 3,5-bisphosphate, a molecule critical for intracellular vesicle trafficking along the endosomal-lysosomal pathway.[3] Previous studies have shown that FIG4 is abundantly expressed during neural development in mice and rats; FIG4 is expressed in neurons and myelin-forming cells in the central and peripheral nervous systems, particularly in spinal ganglia sensory neurons and Schwann cells.[4] Although FIG4 protein and mRNA levels are markedly diminished in neurons of the adult CNS, spinal cord injury induces upregulation of FIG4 in the adult spinal cord, and this is associated with accumulation of lysosomes in neurons and glia.[4] FIG4 knockout mice and rats result in spongiform neurodegeneration with enlarged lysosomal vesicles, defective myelination and juvenile lethality.[5,6] These findings suggest that expression of FIG4 is required for neural development and is necessary to prevent neurodegeneration. Mutations of *FIG4* cause Charcot-Marie-Tooth disease type 4J (CMT4J; MIM 611228), a severe form of peripheral neuropathy.[6,7] Mutations of *FIG4* may also lead to the development of familial and sporadic amyotrophic lateral sclerosis (ALS) (ALS11; MIM 609390).[8] However, the localization of FIG4 in the human nervous system has not yet been immunohistochemically investigated.

Abnormal accumulation and aggregation of disease-specific proteins are common features of several neurodegenerative diseases.[9] Impairment of the endosomal-lysosomal and autophagy-lysosomal pathways